Potassium intercalation in graphite: A van der Waals density-functional study

Eleni Ziambaras,[1] Jesper Kleis,[1] Elsebeth Schröder,[1] and Per Hyldgaard[1,2,*]
[1]*Department of Applied Physics, Chalmers University of Technology, SE-412 96 Göteborg, Sweden*
[2]*Microtechnology and Nanoscience, MC2, Chalmers University of Technology, SE-412 96 Göteborg, Sweden*
(Received 18 April 2007; revised manuscript received 12 August 2007; published 22 October 2007)

Potassium intercalation in graphite is investigated by first-principles theory. The bonding in the potassium-graphite compound is reasonably well accounted for by traditional semilocal density-functional theory (DFT) calculations. However, to investigate the intercalate formation energy from pure potassium atoms and graphite requires use of a description of the graphite interlayer binding and thus a consistent account of the nonlocal dispersive interactions. This is included seamlessly with ordinary DFT by a van der Waals density-functional (vdW-DF) approach [M. Dion *et al.*, Phys. Rev. Lett. **92**, 246401 (2004)]. The use of the vdW-DF is found to stabilize the graphite crystal, with crystal parameters in fair agreement with experiments. For graphite and potassium-intercalated graphite, structural parameters such as binding separation, layer binding energy, formation energy, and bulk modulus are reported. Also, the adsorption and subsurface potassium absorption energies are reported. The vdW-DF description, compared with the traditional semilocal approach, is found to weakly soften the elastic response.

DOI: 10.1103/PhysRevB.76.155425 PACS number(s): 71.20.Tx, 81.05.Uw, 68.43.Bc

I. INTRODUCTION

Graphite with its layered structure is easily intercalated by alkali metals (AMs) already at room temperature. The intercalated compound has two-dimensional layers of AMs between graphite layers,[1–5] giving rise to interesting properties, such as superconductivity.[6,7] The formation of an AM-graphite intercalate proceeds with adsorption of AM atoms on graphite and absorption of AM atoms below the top graphite layer, after which further exposure to AM atoms leads the AM intercalate compound.

Recent experiments[8,9] on the structure and electronic properties of AM/graphite systems use samples of graphite that are prepared by heating SiC crystals to temperatures around ~1400 °C.[10] This heat-induced graphitization[11] is of great value for spectroscopic studies of graphitic systems, since the resulting graphite overlayers are of excellent quality.[12] The nature of the bonding between the SiC surfaces and graphite has been explored experimentally with photoemission spectroscopy[13] and theoretically[14] in a density-functional theory (DFT) approach in which we recently extended the functional to include an account of the nonlocal dispersion or van der Waals (vdW) interactions.[15–19]

Here, we use this van der Waals density-functional (vdW-DF) approach[18] to provide an *ab initio* determination of the potassium-intercalation effects on the graphite structure and elastic response and of the energetics of the intercalation process. The final intercalate compound is C_8K. The AM intercalate system is interesting in itself and has been the focus of numerous experimental investigations.[20–24] Graphitic and graphitic-intercalation systems are also ideal test materials in ongoing theory developments[18,19,25–41] which aim to improve the DFT description of sparse systems containing, for example, nonlocal (vdW) interlayer bonds in graphitic materials.[17,42–44]

The choice of vdW-DF[18] is essential for a meaningful *ab initio* comparison of graphite and C_8K properties and to determine the energetics of the C_8K formation. Standard DFT approaches are based on local [local density approximation (LDA)] and semilocal approximations [generalized gradient approximation (GGA)][45–48] for the electron exchange and correlation. While LDA calculations show some binding between graphite sheets,[49–55] they fail to provide an accurate account of vdW forces.[56] GGA calculations show no relevant minimum for the graphite energy variation with lattice constants.[57] Neither of these traditional functionals can capture the vdW physics[16,18,19] and there is no basis to trust that they can provide a transferable account[16] in soft-matter problems, for example, involving the weak interlayer binding in graphitic materials.[32,35,43,44] Lack of a physics basis is a fundamental limitation of traditional-DFT implementations that makes it impossible to use them to obtain meaningful comparisons of the graphite and AM intercalate properties. In contrast, the vdW-DF method[16–19] has such a physics basis that can provide the transferability necessary for meaningful *ab initio* comparisons in general, soft- and hard-matter, problems.

We use the vdW-DF method for investigations of graphitic and graphitic-intercalation systems such as C_8K not only to obtain a characterization and comparison of the material properties (probing the accuracy of vdW-DF calculations) but also to test the transferability of the vdW-DF method across a broad spectrum of interactions (covalent, vdW, and partly ionic bonding). We explore the nature of the bonding of graphite, the graphite exfoliation, the process leading to intercalation via adsorption and absorption of potassium, and the nature of potassium-intercalated graphite C_8K. We calculate the structure and elastic response (bulk modulus B_0) of pristine graphite and potassium-intercalated graphite and we present results for the formation energies of the C_8K system. The intercalation of potassium in graphite is preceded by the adsorption of potassium on top of a graphite surface and potassium absorption underneath the top graphite layer of the surface, and we compare the calculated energies against experimental observations, noting that the formation of the subsurface absorption involves a graphite exfoliation process. Our vdW-DF investigations of the binding of potassium in or on graphite supplement corresponding vdW-DF

studies of the binding of polycyclic aromatic hydrocarbon dimers, of the polyethylene crystal, of benzene dimers, and of polycyclic aromatic hydrocarbon and phenol molecules on graphite.[43,58–63] The set of vdW-DF calculations thus encompasses problems (such as the binding within the individual graphite sheets) that have a purely covalent nature, problems (such as the interlayer binding in graphitics materials) that have a pronounced vdW component, and problems (such as the AM intercalation) that are partly ionic. The set of vdW-DF comparisons therefore implicitly tests the transferability of the *ab initio* method.

The outline of the paper is as follows. Section II contains a short description of the materials of interest here: graphite, C_8K, and graphite with an adsorbed or absorbed K atom layer. The vdW-DF scheme is described in Sec. III. Section IV presents our results, Sec. V presents the discussion, and conclusions are drawn in Sec. VI.

II. MATERIAL STRUCTURE

Graphite is a semimetallic solid with strong intraplane bonds and weakly coupled layers. The presence of these two types of bonding results in a material with different properties along the various crystallographic directions.[64] For example, the thermal and electrical conductivities along the carbon sheets are 2 orders of magnitude higher than those perpendicular to the sheets. This specific property allows heat to move directionally, which makes it possible to control the heat transfer. The relatively weak vdW forces between the sheets contribute to another industrially important property: graphite is an ideal lubricant. In addition, the anisotropic properties of graphite make the material suitable as a substrate in electronic studies of ultrathin metal films.[65–68]

The natural structure of graphite is an *AB* stacking, with the graphite layers shifted relative to each other, as illustrated in Fig. 1. The figure also shows hexagonal graphite, consisting of *AA*-stacked graphite layers. The in-plane lattice constant a and the layer separation $d_{C\text{-}C}$ are also illustrated. In natural graphite, the primitive unit cell is hexagonal, includes four carbon atoms in two layers, and has unit-cell side lengths a and height $c=2d_{C\text{-}C}$.

The physical properties of graphite have been studied in a variety of experimental[69–71] and theoretical[49–55] works. Some of the DFT studies have been performed in LDA, which does not provide a physically meaningful account of binding in layered systems.[17,32,35,42] At the same time, using GGA is not an option because it does not bind the graphite layers.[57] For a good description of the graphite structure and nature, the vdW interactions must be included.[16]

AMs, except Na, easily penetrate the gallery of the graphite, forming alkali metal graphite intercalation compounds. These intercalation compounds are formed through electron exchange between the intercalated layer and the host carbon layers, resulting in a nature of the interlayer bonding type different from that of pristine graphite. The intercalate also affects the conductive properties of graphite, which becomes superconductive in the direction parallel to the planes at critical temperatures below 1 K.[6,7]

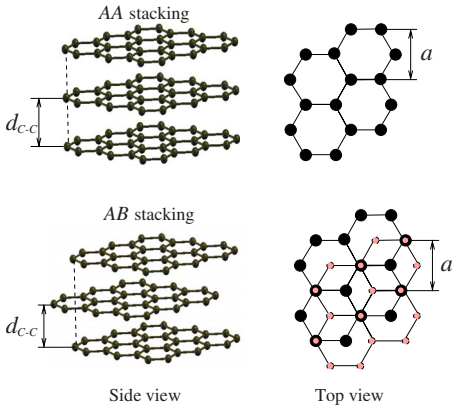

FIG. 1. (Color online) Simple hexagonal graphite (*AA* stacking) and natural hexagonal graphite (*AB* stacking). The two structures differ by that each second carbon layer in *AB*-stacked graphite is shifted, whereas in *AA*-stacked graphite, all planes are directly above each other. The experimentally obtained in-plane lattice constant and sheet separation of natural graphite are (Ref. 69) $a=2.459$ Å and $d_{C\text{-}C}=3.336$ Å, respectively.

The structure of AM-graphite intercalation compounds is characterized by its stage n, where n is the number of graphite sheets located between the AM layers. In this work, we consider only stage-1 intercalated graphite C_8K, in which the layers of graphite and potassium alternate throughout the crystal. The primitive unit cell of C_8K is orthorhombic and contains 16 C atoms and 2 K atoms. In the C_8K crystal, the K atoms are ordered in a $p(2\times2)$ registry with K-K separation $2a$, where a is the in-plane lattice constant of graphite. This separation of the potassium atoms is about 8% larger than that in the natural K bcc crystal (based on experimental values). The carbon sheet stacking in C_8K is of *AA* type, with the K atoms occupying the sites over the hollows of every fourth carbon hexagon, each position denoted by α, β, γ, or δ, and the stacking of the K atoms perpendicular to the planes being described by the $\alpha\beta\gamma\delta$ sequence, as illustrated in Fig. 2.

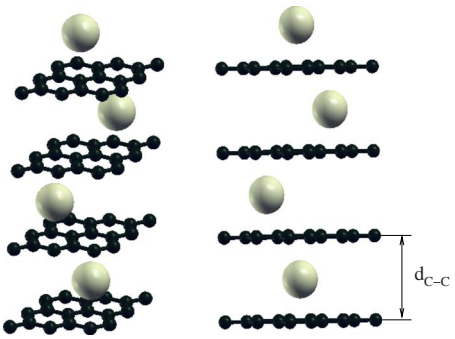

FIG. 2. (Color online) Crystalline structure of C_8K showing the *AA* stacking of the carbon layers (small balls) and the $\alpha\beta\gamma\delta$ stacking of the potassium layers (large balls) perpendicular to the graphene sheets. The potassium layers are arranged in a $p(2\times2)$ structure, with the K atoms occupying the sites over the hollows of every fourth carbon hexagon.

III. COMPUTATIONAL METHODS

The first-principles total-energy and electronic structure calculations are performed within the framework of DFT. The semilocal Perdew-Burke-Ernzerhof (PBE) flavor[46] of GGA is chosen for the exchange-correlation functional for the traditional self-consistent calculations underlying the vdW-DF calculations. For all GGA calculations, we use the open-source DFT code DACAPO,[72] which employs Vanderbilt ultrasoft pseudopotentials,[73] periodic boundary conditions, and a plane-wave basis set. An energy cutoff of 500 eV is used for the expansion of the wave functions and the Brillouin zone (BZ) of the unit cells is sampled according to the Monkhorst-Pack scheme.[74] The self-consistently determined GGA valence electron density $n(\boldsymbol{r})$ as well as components of the energy from these calculations are passed on to the subsequent vdW-DF calculation of the total energy.

We assume a rigid, flat structure of the graphite sheets. This implies that all atoms are kept frozen in calculations where we vary the structural parameters. We stress that individual (graphene) sheets are indeed very unflexible and we expect no significant effects from this approximation, except when resolving very small energy differences.

For the adsorption and absorption studies, a graphite surface slab consisting of four layers is used, with a surface unit cell of side lengths twice those in the graphite bulk unit cell (i.e., side lengths $2a$). The surface calculations are performed with a $4\times4\times1$ k-point sampling of the BZ.

The (pure) graphite bulk GGA calculations are performed with an $8\times8\times4$ k-point sampling of the BZ, whereas for the C_8K bulk structure, in a unit cell at least double the size in any direction, $4\times4\times2$ k points are used, also consistent with the choice of k-point sampling of the surface slabs.

We choose to describe C_8K by using a hexagonal unit cell with 4 formula units (f.u.), lateral side lengths approximately twice those of graphite, and with four graphite and four K layers in the direction perpendicular to the layers. C_8K can also be described by the previously mentioned primitive orthorhombic unit cell containing 2 f.u. of atoms but we retain the orthorhombic cell for ease of description and for simple implementation of our numerically robust vdW-DF calculations.

In all our studies, except test cases, the fast Fourier transform (FFT) grids are chosen such that the separation of neighboring points is maximum ($\sim$0.13 Å) in any direction in any calculation.

A. van der Waals density function calculations

In graphite, the carbon layers bind by vdW interactions only. In the intercalated compound, a major part of the attraction is ionic,[75] but also here the vdW interactions cannot be ignored. In order to include the vdW interactions systematically in all of our calculations, we use the vdW-DF of Ref. 18. There, the correlation energy functional is divided into a local and a nonlocal part,

$$E_c \approx E_c^{\mathrm{LDA}} + E_c^{\mathrm{nl}}, \tag{1}$$

where the local part is approximated in the LDA and the nonlocal part E_c^{nl} is consistently constructed to vanish for a homogeneous system. The nonlocal correlation E_c^{nl} is calculated from the GGA-based $n(\boldsymbol{r})$ and its gradients by using information about the many-body response of the weakly inhomogeneous electron gas:

$$E_c^{\mathrm{nl}} = \frac{1}{2}\int_{V_0} d\boldsymbol{r} \int_V d\boldsymbol{r}'\, n(\boldsymbol{r})\,\phi(\boldsymbol{r},\boldsymbol{r}')\,n(\boldsymbol{r}'). \tag{2}$$

The nonlocal kernel $\phi(\boldsymbol{r},\boldsymbol{r}')$ expresses the (many-electron) density response and respects a wide number of sum rules.[18] The kernel can be tabulated in terms of the separation $|\boldsymbol{r}-\boldsymbol{r}'|$ between the two fragments at positions $\boldsymbol{r}$ and $\boldsymbol{r}'$ through the parameters $D=(q_0+q_0')|\boldsymbol{r}-\boldsymbol{r}'|/2$ and $\delta=(q_0-q_0')/(q_0+q_0')$. Here, q_0 is a local parameter that depends on the electron density and its gradient at position $\boldsymbol{r}$. The analytic expression for the kernel ϕ in terms of D and δ can be found in Ref. 18.

The E_c^{nl} evaluation contains a six dimensional integration in which we use a density cutoff of 10^{-4} a.u. that ensures convergence also in the presence of charge transfer processes (arising in the potassium-graphite systems). Like all density-functional implementations, our vdW-DF uses a density floor to avoid spurious contributions from low-level numeric noise in the calculated density distribution. We use a moderately low cutoff that speeds up the evaluation and we explicitly test that our choice maintains accuracy. In practice, we calculated the graphite exfoliation energies and potassium adsorption energies (both defined below) for a range of different density-cutoff choices to document that our choice, 10^{-4} a.u., converges the vdW-DF adsorption (exfoliation) energy to about 1 meV (to much less than 1 meV) per 33-atom (32-atom) unit cell.

For periodic systems, such as bulk graphite, C_8K, and the graphite surface (with adsorbed or absorbed K atoms), the nonlocal correlation per unit cell is simply evaluated from the interaction of the points in the unit cell V_0 with relevant density points everywhere in space (V) in the three (for bulk graphite and C_8K) or two (for the graphite surface) dimensions of periodicity. Thus, the V integral in Eq. (2), in principle, requires a representation of the electron density infinitely repeated in space. In practice, the nonlocal correlation rapidly converges[43] and it suffices with repetitions of the unit cell a few times in each spatial direction. For graphite bulk, the V integral is converged when we use a V that extends nine (seven) times the original unit cell in directions parallel (perpendicular) to the sheets. For the potassium investigation, a significantly larger original unit cell is adopted (see Fig. 2); here, a fully converged V corresponds to a cell extending five (three) times the original cell in the direction parallel (perpendicular) to the sheets for C_8K bulk. To describe the nonlocal correlations in Eq. (2) for the graphite surface, a sufficient V extends five times the original unit cell along the carbon sheets.

For the exchange energy E_x, we follow the choice of Ref. 18 of using revPBE[47] exchange. Among the functionals that we have easy access to, the revPBE has proved to be the best candidate for minimizing the tendency of artificial exchange binding in graphite.[17]

Using the scheme described above to evaluate E_c^{nl}, the total energy finally reads

$$E^{\mathrm{vdW\text{-}DF}} = E^{\mathrm{GGA}} - E_c^{\mathrm{GGA}} + E_c^{\mathrm{LDA}} + E_c^{\mathrm{nl}}, \tag{3}$$

where E^{GGA} is the GGA total energy with the revPBE choice for the exchange description and E_c^{GGA} (E_c^{LDA}) the GGA (LDA) correlation energy. As our GGA calculations in this specific application of vdW-DF are carried out in PBE, not revPBE, we further need to explicitly replace the PBE exchange in E^{GGA} by that of revPBE for the same electron charge density distribution.

B. Convergence of the local and nonlocal energy variations

DFT calculations provide physically meaningful results for energy differences between total energies (3). To understand materials and processes, we must compare total-energy differences between a system with all constituents at relatively close distance and a system of two or more fragments at "infinite" separation (the reference system). Since total energy (3) consists of both a long-range term and shorter-range GGA and LDA terms, it is natural to choose different ways to represent the separated fragments for these different long- or short-range energy terms.

For the shorter-range energy parts (LDA and GGA terms), the reference system is a full system with vacuum between the fragments. For LDA and GGA calculations, it normally suffices to make sure that the charge density tails of the fragments do not overlap, but here we find that the surface dipoles cause a slower convergence with layer separation. We use a system with the layer separation between the potassium layer and the nearest graphite layer(s) $d_{\mathrm{C\text{-}K}}=12$ Å (8 Å) as reference for the adsorption (absorption) study.

The evaluation of the nonlocal correlations E_c^{nl} requires additional care. This is due to technical reasons pertaining to numerical stability in basing the E_c^{nl} evaluation on the FFT grid used to converge the underlying traditional-DFT calculations. The evaluation of the nonlocal correlation energy, Eq. (2), involves a weighted double integral of a kernel with a significant short-range variation.[18] The shape of the kernel makes the E_c^{nl} evaluation sensitive to the particulars of FFT-type griding,[76] for example, to the relative position of FFT grid points relative to the nuclei position (for a finite grid-point spacing).

However, robust evaluation of binding- or cohesive-energy contributions by nonlocal correlations can generally be secured by a further splitting of energy differences into steps that minimize the above-mentioned grid sensitivity. The problem of FFT sensitivity of the E_c^{nl} evaluation is accentuated because the binding in the E_c^{nl} channel arises as a smaller energy difference between sizable E_c^{nl} contributions of the system and of the fragments. Conversely, convergence in vdW-DF calculations of binding and cohesive energies can be obtained even at a moderate FFT grid accuracy (0.13 Å used here) by devising a calculational scheme that always maintains identical position of the nuclei relative to grid points in the combined systems as well as in the fragment reference system.

Thus, we obtain a numerically robust evaluation of the E_c^{nl} energy differences by choosing steps for which we can explicitly control the FFT griding. For adsorption and absorption cases, we calculate the reference systems as a sum of E_c^{nl} contributions for each fragment and we make sure to always position the fragment at the exact same position in the system as in the interacting system. For bulk systems, we choose steps in which we exclusively adjust the interplane or in-plane lattice constant. Here, the reference system is then simply defined as a system with double (or in some cases quadruple) lattice constant and with a corresponding doubling of the FFT griding along the relevant unit-cell vector.

The cost of full convergence is that, in practice, we often do three or more GGA calculations and subsequent E_c^{nl} calculations for each point on the adsorption, absorption, or formation-energy curve. In addition to the calculations for the full system, we have to do one for each of the isolated fragments at identical position in the adsorption and/or absorption cases and one or more for fragments in the doubled unit cell and doubled griding reference. We have explicitly tested that using a FFT grid spacing of <0.13 Å (but not larger) for such reference calculations is sufficient to ensure full convergence in the reported E_c^{nl} (and $E^{\mathrm{vdW\text{-}DF}}$ total) energy variation for graphitic systems.

C. Material formation and sorption energies

The cohesive energy of graphite (G) is the energy gain, per carbon atom, of creating graphite at in-plane lattice constant a and layer separation $d_{\mathrm{C\text{-}C}}$ from isolated (spin-polarized) carbon atoms.

$$E_{\mathrm{G,coh}}(a,d_{\mathrm{C\text{-}C}}) = E_{\mathrm{G,tot}}(a,d_{\mathrm{C\text{-}C}}) - E_{\mathrm{C\text{-}atom,tot}}, \tag{4}$$

where $E_{\mathrm{G,tot}}$ and $E_{\mathrm{C\text{-}atom,tot}}$ are total energies per carbon atom. The graphite structure is stable at the minimum of the cohesive energy, at lattice constants $a=a_{\mathrm{G}}$ and $2d_{\mathrm{C\text{-}C}}=c_{\mathrm{G}}$.

The adsorption (absorption) energy for a $p(2\times2)$ K layer over (under) the top layer of a graphite surface is the difference in total energy [from Eq. (3)] for the system at hand and the total energy of the initial system, i.e., a clean graphite surface and isolated gas-phase potassium atoms. However, due to the above-mentioned technical issues in using the vdW-DF, we calculate the adsorption and absorption energies as a sum of (artificial) stages leading to the desired system: First, the initially isolated, spin-polarized potassium atoms are gathered into a free-floating potassium layer with the structure corresponding to a full cover of potassium atoms. By this, the total system gains the energy $\Delta E_{\mathrm{K\text{-}layer}}(a_{\mathrm{G}})$, with

$$\Delta E_{\mathrm{K\text{-}layer}}(a) = E_{\mathrm{K,tot}}(a) - E_{\mathrm{K\text{-}atom,tot}}. \tag{5}$$

In *adsorption*, the potassium layer is then simply placed on top of the four-layer (2×2) graphite surface (with the K atoms above graphite hollows) at distance $d_{\mathrm{C\text{-}K}}$. The system thereby gains a further energy contribution $\Delta E_{\mathrm{K\text{-}G}}(d_{\mathrm{C\text{-}K}})$. This leads to an adsorption energy per K atom

$$E_{\mathrm{ads}}(d_{\mathrm{C\text{-}K}}) = \Delta E_{\mathrm{K\text{-}layer}}(a_{\mathrm{G}}) + \Delta E_{\mathrm{K\text{-}G}}(d_{\mathrm{C\text{-}K}}). \tag{6}$$

In *absorption*, the top graphite layer is peeled off the (2×2) graphite surface and moved to a distance far from the remains of the graphite surface. This exfoliation process

costs the system an energy $-\Delta E_{\text{C-G}}=-[E_{\text{tot,C-G}}(d_{\text{C-C}}=c_{\text{G}}/2)-E_{\text{tot,C-G}}(d_{\text{C-C}}\to\infty)]$. At the far distance, the isolated graphite layer is moved into *AA* stacking with the surface, at no extra energy cost. Then, the potassium layer is placed midway between the far-away graphite layer and the remains of the graphite surface. Finally, the two layers are gradually moved toward the surface. At distance $2d_{\text{C-K}}$ between the two topmost graphite layers (sandwiching the K layer), the system has further gained an energy $\Delta E_{\text{C-K-G}}(d_{\text{C-K}})$. The absorption energy per K atom is thus

$$E_{\text{abs}}(d_{\text{C-K}}) = -\Delta E_{\text{C-G}} + \Delta E_{\text{K-layer}}(a_{\text{G}}) + \Delta E_{\text{C-K-G}}(d_{\text{C-K}}). \tag{7}$$

While standard DFT gives no meaningful results for the exfoliation energy $-\Delta E_{\text{C-G}}$, and hence for absorption energy (7), both can be calculated with our vdW-DF method.

Similarly, the C_8K intercalate compound is formed from graphite by first moving the graphite layers far apart accordionlike (and there shift the graphite stacking from *ABA*… to *AAA*… at no energy cost), then changing the in-plane lattice constant of the isolated graphene layers from a_{G} to a, then intercalating K layers (in stacking $\alpha\beta\gamma\delta$) between the graphite layers, and finally moving all the K and graphite layers back like an accordion, with in-plane lattice constant a (which has the value a_{C_8K} at equilibrium).

In practice, a unit cell of four periodically repeated graphite layers is used in order to accommodate the potassium $\alpha\beta\gamma\delta$ stacking. The energy gain of creating a (2×2) graphene sheet from eight isolated carbon atoms is defined similarly to that of the K layer:

$$\Delta E_{\text{C-layer}}(a) = E_{\text{C-layer,tot}}(a) - 8E_{\text{C-atom,tot}}. \tag{8}$$

The formation energy for the C_8K intercalate compound per K atom or f.u., E_{form}, is thus found from the energy cost of moving four graphite layers apart by expanding the (2×2) unit cell to large height, $-\Delta E_{\text{G-acc}}$, the cost of changing the in-plane lattice constant from a_{G} to a in each of the four isolated graphene layers, $4[\Delta E_{\text{C-layer}}(a)-\Delta E_{\text{C-layer}}(a_{\text{G}})]$, the gain of creating four K layers from isolated K atoms, $4\Delta E_{\text{K-layer}}(a)$, plus the gain of bringing four K layers and four graphite layers together in the C_8K structure, $\Delta E_{C_8\text{K-acc}}(a,d_{\text{C-K}})$, yielding

$$E_{\text{form}}(a,d_{\text{C-K}}) = \tfrac{1}{4}[-\Delta E_{\text{G-acc}} + 4\Delta E_{\text{C-layer}}(a) - 4\Delta E_{\text{C-layer}}(a_{\text{G}}) + 4\Delta E_{\text{K-layer}}(a) + \Delta E_{C_8\text{K-acc}}(a,d_{\text{C-K}})]. \tag{9}$$

The relevant energies to use for comparing the three different mechanisms of including potassium (adsorption, absorption, and intercalation) are thus $E_{\text{ads}}(d_{\text{C-K}})$, $E_{\text{abs}}(d_{\text{C-K}})$, and $E_{\text{form}}(a,d_{\text{C-K}})$ at their respective minimum values.

IV. RESULTS

Experimental observations indicate that the intercalation of potassium into graphite starts with the absorption of evaporated potassium into an initially clean graphite surface.[77] This subsurface absorption is preceded by initial, sparse potassium adsorption onto the surface, and proceeds with further absorption into deeper graphite voids. The general view is that the K atoms enter graphite at the graphite step edges.[22] The amount and position of intercalated K atoms are controlled by the temperature and time of evaporation.

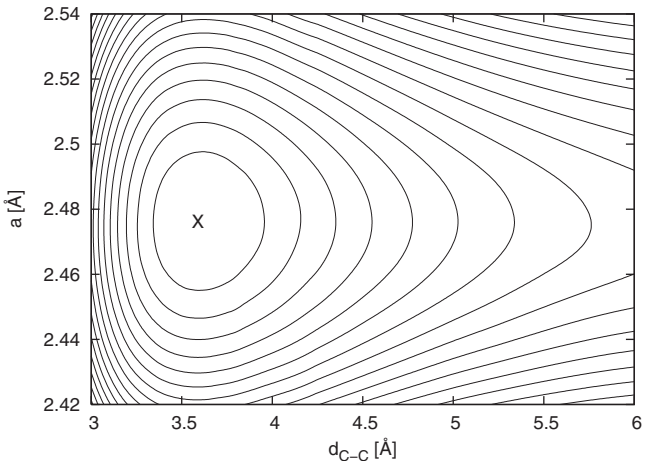

FIG. 3. Graphite cohesive energy $E_{\text{G,coh}}$ (*AB* stacked), based on vdW-DF, as a function of the carbon layer separation $d_{\text{C-C}}$ and the in-plane lattice constant a. The energy contours are spaced by 5 meV per carbon atom.

Below, we first describe the initial clean graphite system and the energy gain in (artificially) creating free-floating K layers from isolated K atoms. Then, we present and discuss our results on potassium adsorption and subsurface absorption, followed by a characterization of bulk C_8K.

For the adsorption (absorption) system, we calculate the adsorption (absorption) energy curve, including the equilibrium structure. As a demonstration of the need for a relatively fine FFT griding in the vdW-DF calculations, we also calculate and compare the absorption curve for a more sparse FFT grid. For the bulk systems (graphite and C_8K), we determine the lattice parameters and the bulk modulus. We also calculate the formation energy of C_8K and the energy needed to peel off one graphite layer from the graphite surface and compare with experiment.[44]

A. Bulk structure and exfoliation of graphite

The present calculations on pure graphite are for the natural, *AB*-stacked graphite (lower panel of Fig. 1). The cohesive energy is calculated at a total of 297 structure values $(a,d_{\text{C-C}})$ and the equilibrium structure and bulk modulus B_0 are then evaluated using the method described in Ref. 78.

Figure 3 shows a contour plot of the graphite cohesive-energy variation $E_{\text{G,coh}}$ as a function of the layer separation $d_{\text{C-C}}$ and the in-plane lattice constant a, calculated within the vdW-DF scheme. The contour spacing is 5 meV per carbon atom, shown relative to the energy minimum located at $(a,d_{\text{C-C}})=(a_{\text{G}},c_{\text{G}}/2)=(2.476\ \text{Å},3.59\ \text{Å})$. These values are summarized in Table I together with the results obtained from a semilocal PBE calculation. As expected, and discussed in Ref. 16, the semilocal PBE calculation yields unrealistic results for the layer separation. The table also pre-

TABLE I. Optimized structure parameters and elastic properties for natural hexagonal graphite (*AB* stacking) and the potassium-intercalated graphite structure C_8K in $A\alpha A\beta A\gamma A\delta A\alpha\ldots$ stacking. The table shows the calculated optimal values of the in-plane lattice constant a, the (graphite-)layer-layer separation $d_{C\text{-}C}$, and the bulk modulus B_0. In C_8K, the value of $d_{C\text{-}C}$ is twice the graphite-potassium distance $d_{C\text{-}K}$.

	Graphite			C_8K		
	PBE	vdW-DF	Expt.	PBE	vdW-DF	Expt.
a (Å)	2.473	2.476	2.459[a]	2.494	2.494	2.480[b]
$d_{C\text{-}C}$ (Å)	$\gg 4$	3.59	3.336[a]	5.39	5.53	5.35[c]
B_0 (GPa)		27	37[d]	37	26	47[d]

[a]Reference 69.
[b]Reference 79.
[c]Reference 4.
[d]Reference 20. Value presented is for C_{33}; for laterally rigid materials, such as graphite and C_8K, C_{33} is a good approximation of B_0.

sents the corresponding experimental values. Our calculated lattice values obtained using the vdW-DF are in good agreement with experiment[69] and close to those found from the older vdW-DF of Refs. 16 and 17 [in which we for E_c^{nl} assume translational invariance of $n(\boldsymbol{r})$ along the graphite planes] at (2.47 Å, 3.76 Å).

Consistent with experimental reports[20] and our previous calculations,[16,17,57] we find graphite to be rather soft, indicated by the bulk modulus B_0 value. Since in-plane compression is very hard in graphite, most of the softness suggested by (the isotropic) B_0 comes from compression perpendicular to the graphite layers, and the value of B_0 is expected to be almost identical to the C_{33} elastic coefficient.[16,20]

Exfoliation is the process of peeling off the topmost graphite sheet from a graphite surface. We calculate the exfoliation energy to be $\Delta E_{C\text{-}G}=-423$ meV per (2×2) unit cell, i.e., −53 per surface carbon atom (Table II). A recent experiment[44] measured the desorption energy of polycyclic aromatic hydrocarbons (basically flakes of graphite sheets) off a graphite surface. From this experiment, the energy cost of peeling off a graphite layer from the graphite surface was deduced to -52 ± 5 meV/atom.

For the energies of the absorbate system and of the C_8K intercalate, a few other graphite-related energy contributions are needed. The energy of collecting C atoms to form a graphene sheet at lattice constant a from isolated (spin-polarized) atoms is given by $\Delta E_{C\text{-layer}}(a)$; we find that changing the lattice constant a from a_G to the equilibrium value a_{C_8K} of C_8K causes this energy to change a mere 30 meV per (2×2) sheet. The contribution $\Delta E_{G\text{-acc}}$ is the energy of moving bulk graphite layers (in this case four periodically repeated layers) far away from each other, by expanding the unit cell along the direction perpendicular to the layers. Thus, $\Delta E_{G\text{-acc}}=32\Delta E_{G,coh}(a_G, c_G/2)-4\Delta E_{C\text{-layer}}(a_G)$, taking the number of atoms and layers per unit cell into account. We find the value $\Delta E_{G\text{-acc}}=-1592$ meV per (2×2) four-layer unit cell. This corresponds to −50 meV per C atom, again consistent with our result for the exfoliation energy, $\Delta E_{C\text{-}G}/8=-53$ meV.

TABLE II. Comparison of the graphite exfoliation energy per surface atom, $E_{C\text{-}G}/8$, graphite-layer binding energy per carbon atom, $\Delta E_{C\text{-acc}}/32$, the energy gain per K atom of collecting K and graphite layers at equilibrium to form C_8K, $\Delta E_{C_8K\text{-acc}}/4$, and the equilibrium formation energy of C_8K, E_{form}.

	$\Delta E_{C\text{-}G}/8$ (meV/atom)	$\Delta E_{C\text{-acc}}/32$ (meV/atom)	$\Delta E_{C_8K\text{-acc}}/4$ (meV/C_8K)	E_{form} (meV/C_8K)
vdW-DF	−53	−50	−793	−873
PBE			−511	
Expt.	-52 ± 5[a]			−1236[b]

[a]Reference 44.
[b]Reference 1.

B. Creating a layer of K atoms

The (artificial) step of creating a layer of potassium atoms from isolated atoms releases a significant energy $\Delta E_{K\text{-layer}}$. This energy contains the energy variation with in-plane lattice constant and the energy cost of changing from a spin-polarized to a spin-balanced electron configuration for the isolated atom.[80]

The creation of the K layer provides an energy gain which is about half an eV per potassium atom, depending on the final lattice constant. With the graphite lattice constant a_G, the energy change, including the spin-change cost, is $\Delta E_{K\text{-layer}}(a_G)=-511$ meV per K atom in vdW-DF (−624 meV when calculated within PBE), whereas with the intercalate lattice constant a_{C_8K}, the energy change is $\Delta E_{K\text{-layer}}(a_{C_8K})=-508$ meV using the vdW-DF.

C. Graphite-on-surface adsorption of potassium

The potassium atoms are adsorbed on a usual *ABA*…-stacked graphite surface. We consider here full (one monolayer) coverage, which is one potassium atom per (2×2) graphite surface unit cell. This orders the potassium atoms in a honeycomb structure with lattice constant $2a_G$ and a nearest-neighbor distance within the K layer of a_G.

The unit cell used in the standard DFT calculations for adsorption and absorption has a height of 40 Å and includes

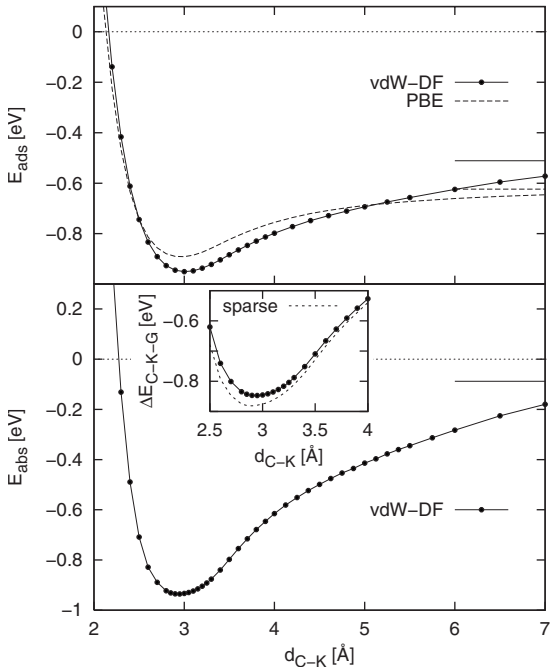

FIG. 4. Potassium adsorption and absorption energies at the graphite surface as a function of the separation $d_{C\text{-}K}$ of the K-atom layer and the nearest graphite layer(s) (at in-plane lattice constant corresponding to that of the surface, a_G). Top panel: Adsorption curve based on vdW-DF calculations (solid line with black circles) and PBE GGA calculations (dashed line). The horizontal lines to the left show the energy gain in creating the isolated K layer from isolated atoms, $\Delta E_{K\text{-layer}}(a_G)$, the asymptote of $E_{ads}(d_{C\text{-}K})$ in this plot. Bottom panel: Absorption curve based on vdW-DF calculations. The asymptote is here the difference $\Delta E_{K\text{-layer}}(a_G) - \Delta E_{C\text{-}G}$. Inset: Binding energy of the K layer and the top graphite layer ("C layer") on top of the graphite slab, $\Delta E_{C\text{-}K\text{-}G}$. The dashed curve shows our results when in E_c^{nl} ignoring every second FFT grid point (in each direction) of the charge density from the underlying GGA calculations, whereas the solid curve with black circles shows the result of using every available FFT grid point.

a vacuum region sufficiently big that no interactions (within GGA) can occur between the top graphene sheet and the slab bottom in the periodically repeated image of the slab. The vacuum region is also large in order to guarantee that the separation from any atom to the dipole layer[81] always remains larger than 4 Å.

In the top panel of Fig. 4, we show the adsorption energy per potassium atom. The adsorption energy at equilibrium is −951 meV per K atom at distance $d_{C\text{-}K}$=3.01 Å from the graphite surface.

For comparison, we also show the adsorption curve calculated in a PBE-only traditional-DFT calculation. Since the interaction between the K layer and the graphite surface has a short-range component to it, even GGA calculations, such as the PBE curve, show significant binding (−892 meV/K atom at $d_{C\text{-}K}$=2.96 Å). This is in contrast to the pure vdW binding between the layers in clean graphite.[16,17] Note that the asymptote of the PBE curve is different from which of the vdW-DF curve, which is due to the different energy gains ($\Delta E_{K\text{-layer}}$) in collecting a potassium layer from isolated atoms when calculated in PBE or in vdW-DF.

For K adsorption, the vdW-DF and PBE curves agree reasonably well, and the use of vdW-DF for this specific calculation is not urgently necessary. However, in order to compare consistently the adsorption results to absorption, intercalation, and clean graphite, it is necessary to include the long-range interactions through vdW-DF. As shown for the graphite bulk results above, PBE yields quantitatively and qualitatively wrong results for the layer separation.

D. Graphite-subsurface absorption of potassium

The first subsurface adsorption of K takes place in the void under the topmost graphite layer. The surface absorption of the first K layer causes a lateral shift of the top graphite sheet, resulting in a *A*/K/*ABAB*… stacking of the graphite. We have studied the bonding nature of this absorption process by considering a full $p(2\times2)$-intercalated potassium layer in the subsurface of a four-layer thick graphite slab.

Following the receipt of Sec. III for absorption energy (7), the energies $\Delta E_{C\text{-}K\text{-}G}$ are approximated by those from a four-layer intercalated graphite slab with the stacking *A*/K/*ABA*, and the values are shown in the inset of Fig. 4. The absorption energy E_{abs} is given by the curve in the bottom panel of Fig. 4, and its minimum is −935 meV per K atom at $d_{C\text{-}K}$ =2.94 Å.

To investigate what grid spacing is sufficiently dense to obtain converged total-energy values in vdW-DF, we do additional calculations in the binding distance region with a more sparse grid. Specifically, the inset of Fig. 4 compares the vdW-DF calculated at full griding with one that uses only every other FFT grid point in each direction, implying a grid spacing for E_c^{nl} (but not for the local terms) which is at most 0.26 Å. We note that using the full grid yields smaller absolute values of the absorption energy. We also notice that the effect is more pronounced for small separations than for larger distances. Thus, given resources, the dense FFT grid calculations are preferred, but even the less dense FFT grid calculations yield reasonably well-converged results. In all calculations (except tests of our graphitic systems), we use a spacing with at most 0.13 Å between grid points. This is a grid spacing for which we have explicitly tested convergence of the vdW-DF for graphitic systems given the computational strategy described and discussed in Sec. III.

E. Potassium-intercalated graphite

When potassium atoms penetrate the gallery of the graphite, they form planes that are ordered in a $p(2\times2)$ fashion along the planes. The K intercalation causes a shift of every second carbon layer, resulting into an *AA* stacking of the graphite sheets. The K atoms then simply occupy the sites over the hollows of every fourth carbon hexagon. The order of the K atoms perpendicular to the planes is described by the $\alpha\beta\gamma\delta$ stacking, illustrated in Fig. 2.

For the potassium-intercalated compound C_8K, we calculate in standard DFT using PBE the total energy at 154 different combinations of the structural parameters a and $d_{C\text{-}C}$. The charge densities and energy terms of these calculations are then used as input to vdW-DF. The equilibrium structure and elastic properties (B_0) both for the vdW-DF results and

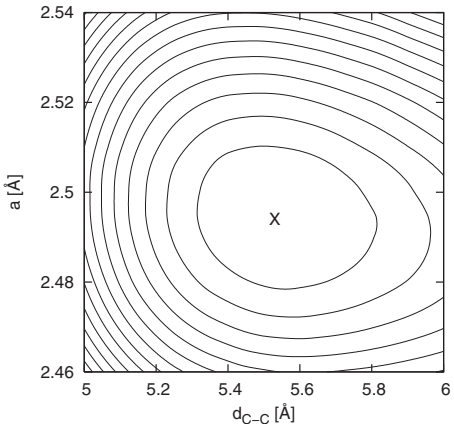

FIG. 5. Formation energy of C_8K, E_{form}, as a function of the graphene-to-graphene layer separation $d_{C\text{-}C}$ and half the in-plane lattice constant a. The energy contours are spaced by 20 meV/f.u.

for the PBE results are then evaluated with the same method as in the graphite case.[78]

Figure 5 shows a contour plot of the C_8K formation energy, calculated in vdW-DF, as a function of the graphene-to-graphene layer separation ($d_{C\text{-}C}$) and the in-plane periodicity (a) of the graphite-layer structure. The contour spacing is 20 meV/f.u. and the contours are shown relative to the energy minimum at $(a, d_{C\text{-}C})=(2.494\ \text{Å}, 5.53\ \text{Å})$.

V. DISCUSSION

Table I presents an overview of our structural results obtained with the vdW-DF for graphite and C_8K. The table also contrasts the results with the corresponding values calculated with PBE where available. The vdW-DF value $d_{C\text{-}C}=5.53$ Å for the C_8K graphene-to-graphene layer separation is 3% larger than the experimentally observed value, whereas the PBE value corresponds to less than a 1% expansion. Our vdW-DF result for the C_8K bulk modulus (26 GPa) is also softer than the PBE result (37 GPa) and further away from the experimental estimates (47 GPa) based on measurements of the C_{33} elastic response.[20] A small overestimation of atomic separation is consistent with the vdW-DF behavior that has been documented in a wide range of both finite and extended systems.[16–19,60–63] This overestimation results, at least in part, from our choice of parametrization of the exchange behavior—an aspect that lies beyond the present vdW-DF implementation which focuses on improving the account of the nonlocal correlations, *per se*. It is likely that systematic investigations of the exchange effects can further refine the accuracy of vdW-DF implementations.[82] In any case, vdW-DF theory calculations represent, in contrast to PBE, the only approach to obtain a full *ab initio* characterization of the AM intercalation process.

The C_8K system is more compact than graphite and this explains why PBE alone can here provide a good description of the materials structure and at least some materials properties, whereas it fails completely for graphite. The distance between the graphene sheets upon intercalation of potassium atoms is stretched compared to that of pure graphite, but the K-layer to graphite-layer separation, $d_{C\text{-}K}=d_{C\text{-}C}/2=2.77$ Å, is significantly less than the layer-layer separation in pure graphite. This indicates that C_8K is likely held together, at least in part, by shorter-range interactions.

TABLE III. Comparison of structure and energies for potassium adsorption, subsurface absorption, and formation of bulk intercalate on and in graphite.

$E_{ads}=-951$ meV/K atom, $d_{C\text{-}K}=3.01$ Å
$E_{abs}=-935$ meV/K atom, $d_{C\text{-}K}=2.94$ Å
$E_{form}=-873$ meV/K atom, $d_{C\text{-}K}=2.77$ Å

Table II documents that the vdW binding nevertheless plays an important role in the binding and formation of C_8K. The table summarizes and contrasts our vdW-DF and PBE results for graphite exfoliation and layer binding energies as well as C_8K interlayer binding and formation energies. The vdW-DF result for the C_8K formation energy is smaller than experimental measurements by 29%, but all the same it represents a physically motivated *ab initio* calculation. In contrast, the C_8K formation energy is simply unavailable in PBE because PBE, as indicated, fails to describe the layer binding in graphite. Moreover, for the comparisons of vdW-DF and PBE that we can make—for example, of the C_8K layer interaction $\Delta E_{C_8K\text{-}acc}$—the vdW-DF is found to significantly strengthen the bonding compared with PBE (from 511 to 793 meV/f.u.).

It is also interesting to note that the combination of shorter-range and vdW bonding components in C_8K yields a layer binding energy that is close to that of the graphite case. In spite of the difference in nature of interactions, we find almost identical binding energies per layer for the case of the exfoliation and accordion in graphite and for the accordion in C_8K. This observation testifies to a perhaps surprising strength of the so-called soft vdW interactions.

In a wider perspective, our vdW-DF permits a comparison of the range of AM-graphite systems from adsorption over absorption to full intercalation and thus a discussion of the intercalation progress (Table III). Assuming a dense 2×2 configuration, we find that the energies for potassium adsorption, subsurface absorption, and bulk intercalation are nearly degenerate. However, we also find an indication that adsorption is slightly preferred over subsurface absorption, in contrast with the experimentally observed behavior.[77] We note that the adsorption and absorption will likely involve different (minor, not presently included) deformations of the graphite sheets. It is reasonable to expect that a future calculation, resting on the ongoing vdW-DF extention[19] and allowing for atomic relaxations specified by consistent vdW-DF forces, will be able to resolve this 2% discrepancy. We find that the potassium absorption may eventually proceed toward full intercalation (bulk absorption), thanks to a significant release of formation energy.

VI. CONCLUSIONS

In summary, we have used a recently developed vdW-DF method[18,19] for an *ab initio* characterization of graphite,

graphite exfoliation, and of the potassium-intercalation process. We have calculated and compared both the structure and elastic response of the graphite and of the C_8K intercalate system. We have furthermore calculated the graphite interlayer bonding energies and thus completed an *ab initio* comparison of the energetics of the potassium-intercalation process including on-surface K adsorption, subsurface K absorption, and full intercalation.

We find that the vdW-DF results for the graphite exfoliation energy are in excellent agreement with experimental results for the graphite exfoliation energy and in fair agreement with experiments on the C_8K formation. Traditional DFT in the GGA only permits calculation of the interlayer bonding (but not of the formation energy) in the C_8K material. We stress that the vdW-DF strengthens this C_8K interlayer binding energy by more than 50% (from 511 to 793 meV/f.u.), indicating that the vdW interaction supplements the ionic bonding in the C_8K material.

The vdW-DF method furthermore allows an *ab initio* comparison of the structural effects and energetics in the intercalation process. Unlike traditional-DFT implementations, the vdW-DF method provides a physics-based account of the vdW interactions and, hence, simultaneously a consistent description of the weakly bonded graphitic and of the (partly ionic) intercalate systems. We find that the vdW-DF results for the structure and values for elastic response are in fair agreement with experiments. We predict that the intercalation process leaves the bulk modulus unchanged, while experiments indicate a moderate hardening. The vdW-DF results for the potassium adsorption and subsurface absorption energies are nearly degenerate but indicate a slight preference for adsorption, in contrast with experimental observations.

ACKNOWLEDGMENTS

We thank D. C. Langreth and B. I. Lundqvist for stimulating discussions. Partial support from the Swedish Research Council (VR), the Swedish National Graduate School in Materials Science (NFSM), and the Swedish Foundation for Strategic Research (SSF) through the consortium ATOMICS is gratefully acknowledged, as well as allocation of computer time at UNICC/C3SE (Chalmers) and SNIC (Swedish National Infrastructure for Computing).

*hyldgaar@chalmers.se

[1] S. Aronson, F. J. Salzano, and D. Ballafiore, J. Chem. Phys. **49**, 434 (1968).
[2] D. E. Nixon and G. S. Parry, J. Phys. D **1**, 291 (1968).
[3] R. Clarke, N. Wada, and S. A. Solin, Phys. Rev. Lett. **44**, 1616 (1980).
[4] M. S. Dresselhaus and G. Dresselhaus, Adv. Phys. **30**, 139 (1981).
[5] D. P. DiVincenzo and E. J. Mele, Phys. Rev. B **32**, 2538 (1985).
[6] N. B. Hannay, T. H. Geballe, B. T. Matthias, K. Andreas, P. Schmidt, and D. MacNair, Phys. Rev. Lett. **14**, 225 (1965).
[7] R. A. Jishi and M. S. Dresselhaus, Phys. Rev. B **45**, 12465 (1992).
[8] T. Kihlgren, T. Balasubramanian, L. Walldén, and R. Yakimova, Surf. Sci. **600**, 1160 (2006).
[9] M. Breitholtz, T. Kihlgren, S.-Å. Lindgren, and L. Walldén, Phys. Rev. B **66**, 153401 (2002).
[10] I. Forbeaux, J.-M. Themlin, and J.-M. Debever, Phys. Rev. B **58**, 16396 (1998).
[11] Please see G. Kern and J. Hafner, Phys. Rev. B **58**, 13167 (1998) for an *ab initio* (LDA-based) molecular-dynamics study of a corresponding surface-graphitization process for diamond (111).
[12] T. Kihlgren, T. Balasubramanian, L. Walldén, and R. Yakimova, Phys. Rev. B **66**, 235422 (2002).
[13] I. Forbeaux, J.-M. Themlin, A. Charrier, F. Thibaudau, and J.-M. Debever, Appl. Surf. Sci. **162-163**, 406 (2000).
[14] E. Ziambaras, Ph.D. thesis, Chalmers, 2006.
[15] H. Rydberg, B. I. Lundqvist, D. C. Langreth, and M. Dion, Phys. Rev. B **62**, 6997 (2000).
[16] H. Rydberg, M. Dion, N. Jacobson, E. Schröder, P. Hyldgaard, S. I. Simak, D. C. Langreth, and B. I. Lundqvist, Phys. Rev. Lett. **91**, 126402 (2003).
[17] D. C. Langreth, M. Dion, H. Rydberg, E. Schröder, P. Hyldgaard, and B. I. Lundqvist, Int. J. Quantum Chem. **101**, 599 (2005).
[18] M. Dion, H. Rydberg, E. Schröder, D. C. Langreth, and B. I. Lundqvist, Phys. Rev. Lett. **92**, 246401 (2004); **95**, 109902(E) (2005).
[19] T. Thonhauser, V. R. Cooper, S. Li, A. Puzder, P. Hyldgaard, and D. C. Langreth, Phys. Rev. B **76**, 125112 (2007).
[20] N. Wada, R. Clarke, and S. A. Solin, Solid State Commun. **35**, 675 (1980).
[21] H. Zabel and A. Magerl, Phys. Rev. B **25**, 2463 (1982).
[22] J. C. Barnard, K. M. Hock, and R. E. Palmer, Surf. Sci. **287-288**, 178 (1993).
[23] K. M. Hock and R. E. Palmer, Surf. Sci. **284**, 349 (1993).
[24] Z. Y. Li, K. M. Hock, and R. E. Palmer, Phys. Rev. Lett. **67**, 1562 (1991).
[25] J. F. Dobson and B. P. Dinte, Phys. Rev. Lett. **76**, 1780 (1996).
[26] J. F. Dobson and J. Wang, Phys. Rev. Lett. **82**, 2123 (1999).
[27] S. Kurth and J. P. Perdew, Phys. Rev. B **59**, 10461 (1999).
[28] J. M. Pitarke and J. P. Perdew, Phys. Rev. B **67**, 045101 (2003).
[29] D. Sanches-Portal, P. Ordejon, E. Artacho, and J. M. Soler, Int. J. Quantum Chem. **65**, 453 (1997).
[30] M. Elstner, P. Hobza, T. Fraunheim, S. Suhai, and E. Kaxiras, J. Chem. Phys. **114**, 5149 (2001); M. Elstner, D. Porezag, G. Jungnickel, J. Elsner, M. Haugk, T. Frauenheim, S. Suhai, and G. Seifert, Phys. Rev. B **58**, 7260 (1998).
[31] X. Wu, M. C. Vargas, S. Nayak, V. Lotrich, and G. Scoles, J. Chem. Phys. **115**, 8748 (2001).
[32] L. A. Girifalco and M. Hodak, Phys. Rev. B **65**, 125404 (2002).
[33] Q. Wu and W. Yang, J. Chem. Phys. **116**, 515 (2002).
[34] T. Miyake, F. Aryasetiawan, T. Kotani, M. van Schilfgaarde, M. Usuda, and K. Terakura, Phys. Rev. B **66**, 245103 (2002).
[35] M. Hasegawa and K. Nishidate, Phys. Rev. B **70**, 205431 (2004).
[36] S. Grimme, J. Comput. Chem. **25**, 1463 (2004).
[37] U. Zimmerli, M. Parrinello, and P. Koumoutsakos, J. Chem. Phys.

120, 2693 (2004).
[38] X. Xu and W. A. Goddard III, Proc. Natl. Acad. Sci. U.S.A. **101**, 2673 (2004); J. T. Su, X. Xu, and W. A. Goddard III, J. Phys. Chem. A **108**, 10518 (2004).
[39] H. J. Williams and C. F. Chabalowski, J. Phys. Chem. **105**, 646 (2001).
[40] A. J. Misquitta, B. Jeziorski, and K. Szalewicz, Phys. Rev. Lett. **91**, 033201 (2003).
[41] R. Podeszwa and K. Szalewicz, Chem. Phys. Lett. **412**, 488 (2005).
[42] A. Marini, P. Garcia-Gonzalez, and A. Rubio, Phys. Rev. Lett. **96**, 136404 (2006).
[43] S. D. Chakarova-Käck, E. Schröder, B. I. Lundqvist, and D. C. Langreth, Phys. Rev. Lett. **96**, 146107 (2006).
[44] R. Zacharia, H. Ulbricht, and T. Hertel, Phys. Rev. B **69**, 155406 (2004).
[45] J. P. Perdew, J. A. Chevary, S. H. Vosko, K. A. Jackson, M. R. Pederson, D. J. Singh, and C. Fiolhais, Phys. Rev. B **46**, 6671 (1992).
[46] J. P. Perdew, K. Burke, and M. Ernzerhof, Phys. Rev. Lett. **77**, 3865 (1996).
[47] Y. Zhang and W. Yang, Phys. Rev. Lett. **80**, 890 (1998).
[48] B. Hammer, L. B. Hansen, and J. K. Nørskov, Phys. Rev. B **59**, 7413 (1999).
[49] N. A. W. Holzwarth, S. G. Louie, and S. Rabii, Phys. Rev. B **26**, 5382 (1982).
[50] M. T. Yin and M. L. Cohen, Phys. Rev. B **29**, 6996 (1984).
[51] H. J. F. Jansen and A. J. Freeman, Phys. Rev. B **35**, 8207 (1987).
[52] M. C. Schabel and J. L. Martins, Phys. Rev. B **46**, 7185 (1992).
[53] R. Ahuja, S. Auluck, J. Trygg, J. M. Wills, O. Eriksson, and B. Johansson, Phys. Rev. B **51**, 4813 (1995).
[54] I.-H. Lee and R. M. Martin, Phys. Rev. B **56**, 7197 (1997).
[55] J. C. Boettger, Phys. Rev. B **55**, 11202 (1997).
[56] J. M. Pérez-Jordá and A. D. Becke, Chem. Phys. Lett. **233**, 134 (1995).
[57] H. Rydberg, N. Jacobson, P. Hyldgaard, S. I. Simak, B. I. Lundqvist, and D. C. Langreth, Surf. Sci. **532-535**, 606 (2003).
[58] S. D. Chakarova and E. Schröder, Mater. Sci. Eng., C **25**, 787 (2005).
[59] S. D. Chakarova-Käck, Ø. Borck, E. Schröder, and B. I. Lundqvist, Phys. Rev. B **74**, 155402 (2006).
[60] A. Puzder, M. Dion, and D. C. Langreth, J. Chem. Phys. **124**, 164105 (2006).
[61] T. Thonhauser, A. Puzder, and D. C. Langreth, J. Chem. Phys. **124**, 164106 (2006).
[62] S. D. Chakarova-Käck, J. Kleis, and E. Schröder, Chalmers Applied Physics Report No. 2005-16, 2005 (unpublished).
[63] J. Kleis, B. I. Lundqvist, D. C. Langreth, and E. Schröder, Phys. Rev. B **76**, 100201(R) (2007).
[64] D. D. L. Chung, J. Mater. Sci. **37**, 1475 (2002).
[65] M. Breitholtz, T. Kihlgren, S.-Å. Lindgren, H. Olin, E. Wahlström, and L. Walldén, Phys. Rev. B **64**, 073301 (2001).
[66] Z. P. Hu, N. J. Wu, and A. Ignatiev, Phys. Rev. B **33**, 7683 (1986).
[67] J. Cui, J. D. White, R. D. Diehl, J. F. Annett, and M. W. Cole, Surf. Sci. **279**, 149 (1992).
[68] L. Österlund, D. V. Chakarov, and B. Kasemo, Surf. Sci. **420**, L437 (1991).
[69] Y. Baskin and L. Meyer, Phys. Rev. **100**, 544 (1955).
[70] W. Eberhardt, I. T. McGovern, E. W. Plummer, and J. E. Fischer, Phys. Rev. Lett. **44**, 200 (1980).
[71] A. R. Law, J. J. Barry, and H. P. Hughes, Phys. Rev. B **28**, 5332 (1983).
[72] Open-source plane-wave DFT computer code DACAPO, http://www.fysik.dtu.dk/CAMPOS/
[73] D. Vanderbilt, Phys. Rev. B **41**, 7892 (1990).
[74] H. J. Monkhorst and J. D. Pack, Phys. Rev. B **13**, 5188 (1976).
[75] As revealed by explicit calculations of the K-to-graphite charge transfer (unpublished).
[76] D. C. Langreth (private communication); J. Kleis and P. Hyldgaard (unpublished).
[77] The transition from on-surface adsorption to subsurface absorption is identified in experiment by a work function change (Refs. 22 and 23).
[78] E. Ziambaras and E. Schröder, Phys. Rev. B **68**, 064112 (2003).
[79] D. E. Nixon and G. S. Parry, J. Phys. C **2**, 1732 (1969).
[80] O. Gunnarsson, B. I. Lundqvist, and J. W. Wilkins, Phys. Rev. B **10**, 1319 (1974). Since no spin-polarized version of vdW-DF exists at present, we calculate the energy cost for changing the spin of isolated potassium atoms in PBE. The spin-change cost is thus determined to be 26 meV/K atom.
[81] L. Bengtsson, Phys. Rev. B **59**, 12301 (1999), and references therein.
[82] The choice of exchange flavor in vdW-DF was set in Ref. 17 to avoid artificial bonding in noble-gas systems and to better mimic exact exchange calculations for those systems. However, it is far from certain and even unlikely that the conclusions drawn for noble-gas systems carry over to bonding separations smaller than 3 Å.